Role of Phenolic Derivatives in Photopolymerization of an Acrylate Coating

M. DOSSOT,[1] M. SYLLA,[2] X. ALLONAS,[1] A. MERLIN,[2] P. JACQUES,[1] J.-P. FOUASSIER[1]

[1] Département de Photochimie Générale, UMR CNRS No. 7525, Ecole Nationale Supérieure de Chimie, 3 rue Alfred Werner, F-68093 Mulhouse Cedex, France

[2] Laboratoire Etudes et Recherches sur le Matériau Bois, Université Henri Poincaré-Nancy I, BP 239, 54506 Vandoeuvre-lès-Nancy, France

Received 25 May 1999; revised 30 September 1999

ABSTRACT: The photopolymerization of acrylate resins on wood surfaces suffers from retardation and inhibition effects due to the phenolic derivatives present at the interface. This article details the study of the effect of a set of phenolic compounds on the initiation step. The global effect was recorded by differential scanning calorimetry and photocalorimetry. A comparison between a direct photocleavable initiator such as 2,2-dimethyloxy-2-phenylacetophenone (DMPA) and a two-component system like benzophenone/*N*-methyldiethanolamine (BP/MDEA) suggests that the retardation effect observed in the latter case is due to the interaction between phenols and the triplet state of BP. Subsequently, nanosecond transient absorption (NTA) spectroscopy was used to measure in acetonitrile the quenching rate constants k_Q. A hydrogen abstraction occurred, and the ketyl radical quantum yield was also determined by NTA experiments. In comparison with the photoreduction mechanisms proposed in the literature, the high k_Q values obtained were tentatively correlated to the half-wave oxidation potentials of phenols in order to discuss the involvement of an electron transfer within the reaction. Some EPR experiments were done to confirm *in situ* the photoreduction process at the wood surface and the creation of phenoxyl radicals. The interaction of phenols with some initiating radicals was also studied. © 2000 John Wiley & Sons, Inc. J Appl Polym Sci 78: 2061–2074, 2000

Key words: photopolymerization; UV-curing; phenols; wood; photoinitiator

INTRODUCTION

The UV curing of coatings on wood materials has become more and more important, especially for furniture protection.[1–3] At the present time, unsaturated polyesters are widely used as monomers in formulations.[4,5] However, to move toward tighter European VOC (volatile organic contents) legislation requires the search for systems with a lower emission of organic compounds.[6] That is why acrylate monomers are increasing in importance and seem to be further replacing polyesters.[2,4]

The radical polymerization of UV-curing varnishes is inhibited and retarded when coating is made on wood materials rich in extractable substances.[7] The delay in photocuring may prevent industrial work. Besides, some wood-extractable substances have been used to stabilize monomers such as butadiene, isoprene, and methylmethacrylate (MMA).[8–11] The delay of radical polymerization has been attributed to phenolic com-

Correspondence to: J.-P. Fouassier

Journal of Applied Polymer Science, Vol. 78, 2061–2074 (2000)

pounds present in great amounts in the extracts of some wood species.[12–14] The inhibition and retardation activities of several phenolic derivatives have been studied in particular, especially in the case of the thermal polymerization of MMA and styrene.[12–15] It should be noted that these activities occurred in working conditions with an ambient atmosphere: the inhibiting properties of oxygen can thus also affect polymerization.

Still, in the presence of oxygen, some studies have shown that the photopolymerization of acrylate resins is inhibited by phenol.[16–18] A high concentration of α-tocopherol under ambient atmosphere inhibits the photopolymerization of MMA initiated by benzoinethylether, while at low concentration it does not prevent initiation.[16] Phenols combined with oxygen can also inhibit the photopolymerization of a mixture of acrylates initiated by 2,2-dimethoxy-2-phenylacetophenone (DMPA)[17] or the photocrosslinking with the same photoinitiator of a film made in an epoxyacrylate and two monofunctional monomers (isobornylacrylate and *N*-vinylpyrrolidone).[18] To our knowledge, no work was done about the inhibition activity of phenols on the photopolymerization of a vinylic monomer in deoxygenated media.

In this work, various aspects of the polymerization of trimethylolpropane triacrylate (TMPTA) in the presence of phenols were examined in deoxygenated media. First a comparison was drawn between thermal and photochemical processes by using differential scanning calorimetry (DSC) and photocalorimetry (DSP). Thermal initiation was achieved with azobisisobutyronitrile (AIBN). Two photoinitiating processes were examined: the direct photocleavage of DMPA and the photoreduction of benzophenone (BP) by *N*-methyldiethanolamine (MDEA). The global effect of phenols on the total enthalpy change of the reaction and the rate of crosslinking has been demonstrated; the inhibition and retardation effects were examined. Subsequently the interactions between the triplet state ^{3}BP and a set of phenols, which can be considered as models of wood phenolic extracts, were probed by nanosecond transient absorption (NTA) spectroscopy. The quenching rate constants k_Q of ^{3}BP were determined. A photoreduction process occurred, and the quantum yield Φ_{RAD} of ketyl radicals produced inside the reaction was measured. In relation to hydrogen abstraction mechanisms proposed in the literature, the involvement of a charge transfer was suspected. As a consequence, the kinetic data has been tentatively correlated to the half-peak oxidation potential of phenols; and that mechanism is discussed here. The photoreduction of BP by phenolic derivatives has been confirmed *in situ* at the wood surface by EPR detection of phenoxyl radicals in wood samples coated with a photopolymerizable formulation and irradiated in the UV range. Finally, the possible interaction of phenols with several initiating radicals will be briefly examined in this article.

EXPERIMENTAL

Differential Scanning Calorimetry and Photocalorimetry

The photocalorimeter was made using a Perkin Elmer DSC 7 differential scanning calorimeter for which the sample and reference were irradiated with a continuum Xenon UV lamp Osram XBO 450W. A Pyrex filter, cutting the wavelengths under 310 nm, avoided direct excitation of the monomer and phenolic derivatives used. The polymerization of TMPTA 3.7 mol L^{-1} was initiated either in a photochemical or thermal manner. Two photoinitiating systems were used: DMPA at 2×10^{-2} mol L^{-1} and an equimolar mixture of BP and MDEA 2×10^{-2} mol L^{-1}. Irradiation was maintained for 5 min. Thermal initiation was achieved with azobisisobutyronitrile (AIBN) at 2×10^{-2} mol L^{-1}. In all experiments, the four phenols studied (phenol, vanillin, 2,6-dimethoxyphenol, and eugenol) were introduced at 5×10^{-2} mol L^{-1}. The purge gas used was always dry nitrogen to avoid oxygen inhibition. All the samples and the apparatus lay under a glove box filled with nitrogen.

The thermograms were recorded at 25°C (298 K) for photochemical polymerization and at 110°C (383 K) for the thermal version. The photopolymerization process requires open cells for irradiation; as a consequence, it is not possible to reach temperatures more than 75°C (348 K) for the evaporation of TMPTA and the loss of weight. The integration of thermograms gives the time evolution of the enthalpy change of the reaction, written as $\Delta H(t)$. Typical traces can be seen for instance in Figure 1. $\Delta H(t)$ starts to increase linearly after a longer or shorter induction period and levels off at the end of the polymerization. The total amount of enthalpy change, ΔH_g, which corresponds to the enthalpy change obtained at the end of the polymerization, that is, at the plateau value, is related to the maximum degree of

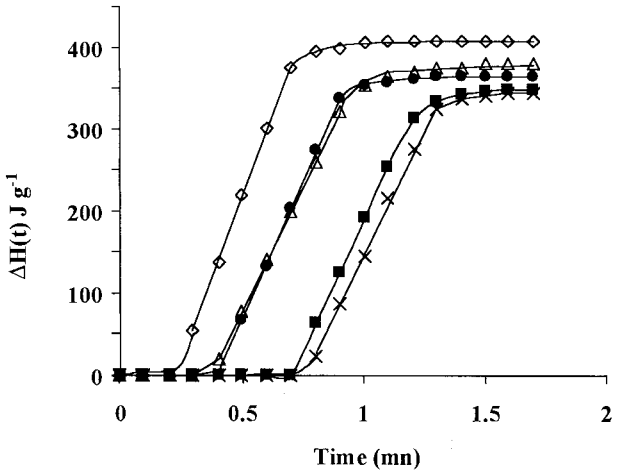

Figure 1 Influence of phenolic derivatives on the thermal polymerization of TMPTA initiated by AIBN. (◇): reference TMPTA + AIBN. (●), (△), (■), and (×): addition of, respectively, phenol, vanillin, 2,6-dimethoxyphenol, and eugenol. Temperature is set to 383 K (110°C).

crosslinking and was actually determined after 5 min. Regarding all the curves collected in Figure 1, it may reasonably be considered that the reaction has finished at this time. The increase slope of $\Delta H(t)$ corresponds to the rate of polymerization. If an additive lowers this slope, the polymerization is said to be retarded. If a delay is observed at the start of the polymerization, the polymerization is said to be inhibited, and the delay is called the "induction period." To make valuable comparisons among the three systems studied, it is useful to divide the value of ΔH_g found for a given phenolic additive ($\Delta H_g(P)$) by the value obtained for the system without phenol ($\Delta H_g^{\mathrm{REF}}$). A parameter, R, is defined by eq. (1):

$$R = \frac{\Delta H_g(P)}{\Delta H_g^{\mathrm{REF}}} \tag{1}$$

Nanosecond Transient Absorption Spectroscopy

The quenching rate constants, k_Q, and the ketyl radical quantum yields, Φ_{RAD}, were measured by NTA spectroscopy. The excitation source was a frequency triplet Q-switched Nd : YAG laser (B. M. Industries) generating 9 ns pulses of 20 mJ at 355 nm. A pulsed xenon lamp (OSRAM XBO 450W) was used at a right angle as the monitoring beam, focused on the entrance slit of a monochromator. A photomultiplier tube (Hamamatsu IP 28) was attached to the exit slit of the monochromator. The signal fed into a transient digitizer (Tektronix DSA 601A). All the data were collected and analyzed, using a PC computer and software developed by our laboratory. All the solutions were made in neat acetonitrile (Fluka spectrophotometric grade). The concentration of BP was 5×10^{-3} mol L^{-1} in order to have an absorbance near 0.5 at the excitation wavelength (355 nm). Oxygen was removed by bubbling argon for 15 min. The values of the quenching rate constants were obtained from the measurements of the transient absorption decay of ^{3}BP at 525 nm[19] by applying the Stern–Volmer analysis. All the Stern–Volmer plots of the collected data were linear.

In order to avoid a possible overlap with the triplet band, the decay of the ketyl radical BPH• was followed at 560 nm rather than at its maximum absorption in acetonitrile, at 545 nm.[20] The molecular extinction coefficients of ^{3}BP and BPH• are respectively $\varepsilon_{525}(^3\mathrm{BP}) = 6500$ M^{-1} cm^{-1} and $\varepsilon_{545}(\mathrm{BPH}\bullet) = 4600$ M^{-1} cm^{-1} in acetonitrile at 525 nm and 545 nm, respectively.[20] From the recorded transient absorption spectra it was thus determined that $\varepsilon_{560}(\mathrm{BPH}\bullet)$ is equal to 2580 M^{-1} cm^{-1}. The ketyl radical quantum yield Φ_{RAD} is given by eq. (2):

$$\Phi_{\mathrm{RAD}} = \frac{[\mathrm{BPH}\bullet]}{[^3\mathrm{BP}]} = \frac{\varepsilon_{525}(^3\mathrm{BP})}{\varepsilon_{560}(\mathrm{BPH}\bullet)} * \frac{A_{560}(\mathrm{BPH}\bullet)}{A_{525}(^3\mathrm{BP})} \tag{2}$$

where $A_{525}(^3\mathrm{BP})$ and $A_{560}(\mathrm{BPH}\bullet)$ stand respectively for the initial absorbance of ^{3}BP and BPH• at the subscripted wavelengths.

Cyclic and Rotating Disk Electrode Voltammetries

Oxidation potentials of phenols were measured in argon-saturated acetonitrile solutions by cyclic (CV) and rotating-disk electrode (RDEV) voltammetries compared to a saturated calomel electrode (SCE) in methanol used as the reference electrode. The reference electrode is connected to the sample solution through a fritted glass bridge containing the supporting electrolyte solution. The potential of this electrode, confirmed by using ferrocene as the internal standard in some experiments, was taken as +0.249/NHE. A 0.1 mol L^{-1} *tert*-butylammonium hexafluorophosphate solution (Fluka electrochemical grade recrystallized in a ethanol–water mixture) was used as the supporting electrolyte. Concentrations of phenolic derivatives were 5×10^{-3} mol L^{-1} in CV and 5 to 20

$\times 10^{-3}$ mol L^{-1} in RDEV. The system of three electrodes employed is based on a Metrohm Polarecord E506 associated with a VA612 scanner, which allows sweep rates up to 100 V s^{-1} in cyclic voltammetry. The polarographic stand VA663 was fitted with its rotating platinum or gold accessories. The scale of potential explored in CV was −1.9 V/SCE to +1.9 V/SCE, with the sweep rate varying from 0.2 to 2 V s^{-1}. For RDEV the working electrode was only a platinum electrode, and the sweep rate was 5 mV s^{-1}. The RDE voltammograms were treated by a logarithmic analysis based on the equation of polarographic curves.

Electron Paramagnetic Resonance

The EPR apparatus was a Bruker ER 200 D coupled with a data acquisition station (Stellar). Frequency was 9.64 GHz, the central magnetic field was 3450 G, and the sweep covered 100 G. The spectra were recorded at room temperature, and their position was marked out to the signal of the 1,1-diphenyl-2-picrylhydrazyl (DPPH•) radical. The kinetic of the formation of radicals was followed during 1 h. Wood samples (1 × 1 × 30 mm) were irradiated during 1 h by the xenon lamp Osram XBO 1000W, using a Pyrex filter to cut the wavelengths under 310 nm. They were impregnated for 15 min by a solution of initiators in a mixture of water–acetone (v/v 30 : 70). Three photoinitiators were studied: DMPA, benzoinisopropylether (BIE), and the equimolar mixture BP/MDEA. Two wood species were chosen: Norway maple (*Acer pseudoplatanus* L.) and European spruce (*Picea abies* Karst.).

The following notations were used: I_∞ was the intensity of the EPR signal when the concentration of radicals was stationary under UV irradiation, I_0 was the initial intensity due to the absorption of visible light, and $I(t)$ was the intensity at time t. Intensities are proportional to the concentration of radicals. Two parameters were next defined as follows: $A(t) = I_\infty - I(t)$, $\rho = \frac{I_\infty - I_0}{I_0}$. The quantity $A(t)$ follows a first-order kinetic with a rate constant k: $\frac{dA(t)}{dt} = -kdt$. The experimental points were thus fitted by a first-order kinetic law using root-mean squares analysis. The ρ parameter defined the increase of the concentration of radicals under UV-irradiation relative to the concentration observed under visible light exposure. It does not depend on the gain of the apparatus.

Chemicals

BP from Fluka (best-available grade) was sublimated once prior to use. Acetonitrile (Fluka Spectrophotometric grade), DMPA, and MDEA (Aldrich 99+%) were used as received. TMPTA from Aldrich (technical grade) was washed by a water solution of NaOH 5% and dried under $CaCl_2$ to eliminate the inhibitor. AIBN [2,2′-azobis(2-methyl-propionitrile)] from Aldrich (98%) was recrystallized in methanol and stored at 4°C. Phenol, guaiacol (2-methoxyphenol), 2,6-dimethoxyphenol, eugenol (4-allyl-2-methoxyphenol), sinapinic acid (3,5-dimethoxy-4-hydroxycinnamic acid), syringaldehyde (4-hydroxy-3,5-dimethoxybenzaldehyde), syringic acid (4-hydroxy-3,5-dimethoxybenzoic acid), (±)-catechin hydrate (*trans*-3,3′,4′,5,7-pentahydroxyflavone hydrate), gallic acid monohydrate (3,4,5-trihydroxybenzoic acid monohydrate), vanillin (4-hydroxy-3-methoxybenzaldehyde), and coniferylaldehyde (4-hydroxy-3-methoxycinnamaldehyde) were provided by Aldrich at the best-available grade (98% or 99+%) and were used without further purification. *trans*-4-Hydroxystilbene came from Lancaster (98%) and was used as received.

The set of phenols models phenolic derivatives extracted from wood. Guaiacol, syringic acid, syringaldehyde, and 2,6-dimethoxyphenol stand for typical structures found in the hydrolysis products of wood polyphenolic constituents such as tannins and lignin.[21] Catechin models flavonoid compounds that are widely distributed in wood.[21] Coniferous and deciduous trees also contain several phenols with low molecular weight, especially some monophenols such as eugenol, guaiacol, vanillin, syringaldehyde, and *trans*-4-hydroxystilbene or a polyphenol such as gallic acid. Coniferylaldehyde is found more specifically in coniferous wood extracts.[21]

RESULTS AND DISCUSSION

Effect of Phenols on Polymerization of TMPTA

Phenols are known to affect the propagation and termination steps of radical polymerization reactions.[22] They have no retardation effect on the thermal initiation process[15] but may show another behavior with photochemical initiation. Three initiating systems were selected to make a comparison of some of the global changes in the polymerization of TMPTA. The thermal initiator was AIBN. The first photoinitiator was DMPA, which works according to a fast cleavage pro-

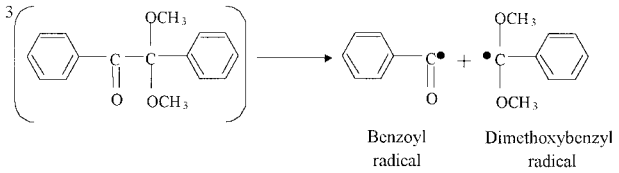

Scheme 1

cess,[23] as shown in Scheme I. The second photoinitiating system was an equimolar mixture of BP and MDEA. In this latter case, a fast hydrogen transfer occurs within a contact ion pair produced by an electron transfer and gives the initiating radicals,[23] as shown in Scheme II.

The evolution of the partial enthalpy change, $\Delta H(t)$, with time for the three systems is shown in Figures 1, 2, and 3. Table I summarizes the values of ΔH_g and parameter R for all the curves. It is noticeable that ΔH_g, and thus the degree of crosslinking, decreases by a factor of 4 from AIBN to BP–MDEA initiating system. To take into account the temperature difference, ΔH_g was measured at three temperatures for the two photoinitiating systems. For technical reasons it was not possible to make the measurements beyond 348 K (see experimental section). Data are compiled in Table II. They are rather well fitted by eq. (3), and Table III gives the values of parameters A and B and the estimated value of ΔH_g at 383 K. This value is calculated by eq. (3), but that 383 K is clearly above the temperature range explored to establish this equation leads us to consider the value obtained as just an estimation. Although the temperature has been taken into account, the crosslinking rate is lower for the two photoinitiating systems compared to AIBN. However, the difference between BP–MDEA and DMPA almost vanishes because of the higher increase of ΔH_g observed with BP–MDEA.

$$\text{Ln } \Delta H_g = A - \frac{B}{T} \tag{3}$$

A look at the parameter R reveals that DMPA and AIBN have nearly the same behavior and the

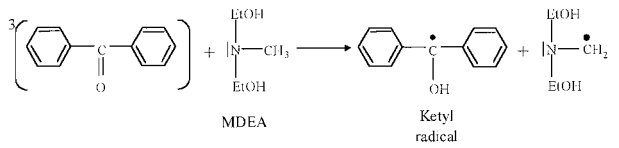

Scheme 2

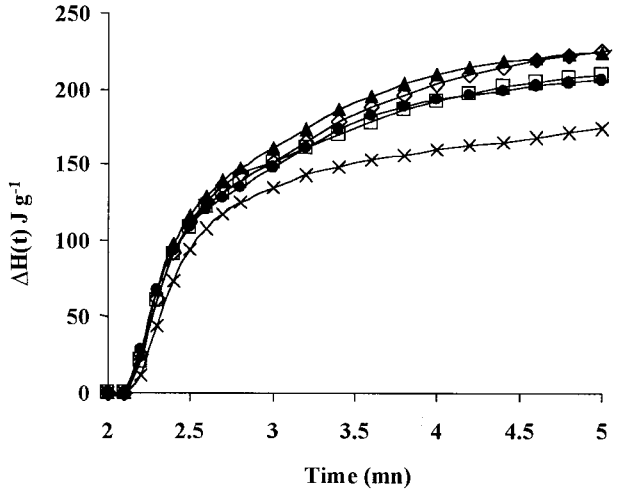

Figure 2 Influence of phenolic derivatives on the photochemical polymerization of TMPTA initiated by DMPA. (◇): reference TMPTA + DMPA. (●), (▲), (□), and (×): addition of, respectively, phenol, vanillin, 2,6-dimethoxyphenol, and eugenol. Temperature is set to 298 K (25°C).

average value of R is about 0.9. Only the BP–MDEA system leads to a marked difference, in that two phenols—2,6-dimethoxyphenol and eugenol—clearly induce a loss of reactivity and have an R value of 0.5. Phenols thus reduce the crosslinking of TMPTA in the three kinds of ini-

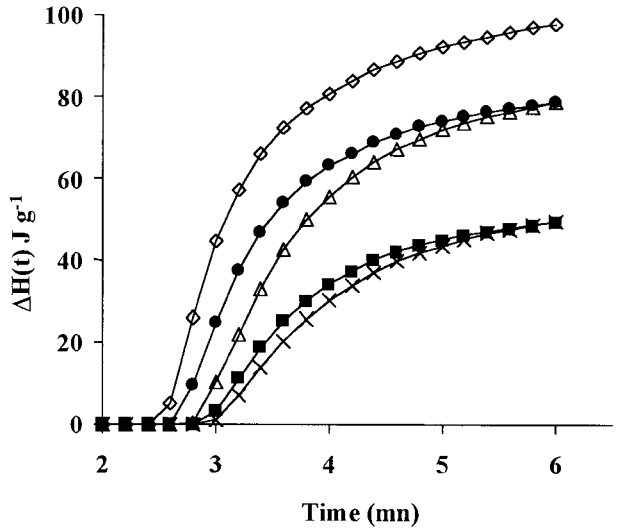

Figure 3 Influence of phenolic derivatives on the photochemical polymerization of TMPTA initiated by BP–MDEA. (◇): reference TMPTA + BP–MDEA. (●), (△), (■), and (×): addition of respectively phenol, vanillin, 2,6-dimethoxyphenol, and eugenol. Temperature is set to 298 K (25°C).

Table I Values of Total Enthalpy Change, ΔH_g, of TMPTA Polymerization for Three Initiating Systems

	System[a]	ΔH_g (J g^{-1})	R
Thermal	AIBN	408	1.00
	AIBN + P	364	0.89
	AIBN + V	381	0.93
	AIBN + DMP	352	0.86
	AIBN + E	346	0.85
Photochemical direct cleavage	DMPA	245	1.00
	DMPA + P	210	0.86
	DMPA + V	230	0.94
	DMPA + DMP	216	0.88
	DMPA + E	185	0.75
Photochemical electron followed by proton transfer	BP–MDEA	97.9	1.00
	BP–MDEA + P	78.7	0.80
	BP–MDEA + V	78.9	0.80
	BP–MDEA + DMP	49.4	0.50
	BP–MDEA + E	49.2	0.50

See experimental section for the definition of parameter R.
[a] Abbreviations are P for phenol, V for vanillin, DMP for 2,6-dimethoxyphenol, and E for eugenol.

tiation, but this effect is enhanced in the case of the BP–MDEA photoinitiator.

From considering the shape of the curves in Figures 1, 2, and 3, it is clear that the three initiating systems lead to three different behaviors. In thermal polymerization, phenols induce a noticeable induction period but no retardation effect. The photoinitiation with DMPA seems to be unaffected by the presence of phenolic derivatives. Indeed, no retardation and a very small induction period, possibly due to the residual oxygen, are detected. Contrary to these observations, the two-component BP–MDEA photoinitiator shows an induction period as in the case of AIBN and, more interestingly, has a markedly retardating effect. Inhibition and retardation effects can lie in the interaction of phenols either with the free radicals produced in the initiation step or with the photoexcited initiators. Phenols are known to scavenge AIBN free radicals,[15] and the induction period observed in Figure 1 confirms this inhibition in deoxygenated media. The inhibition is also observed with the BP–MDEA photoinitiator but not with DMPA. As a consequence, the initiating radicals are not significantly scavenged by phenols in this latter case. The most interesting point arising from these experiments is the retardation effect specifically observed in the BP–MDEA system, while inside the three formulations only the initiator changes. This rules out an interaction of phenols with the propagating radicals; otherwise a retardation should be noticed in the three cases. So the effect with BP–MDEA could be interpreted as an interaction between phenols and the primary species of the photopolymerization, that is, ^{3}BP or the initiating radicals. It is thus important to study and compare the interactions of phenolic derivatives with (1) the triplet states of BP and DMPA and (2) the primary radicals produced in each case.

Table II Evolution with Temperature of Total Enthalpy Change, ΔH_g, of TMPTA Photopolymerization

Temperature T (K)	ΔH_g (J g^{-1})		
	BP–MDEA	BP–MDEA + E[a]	DMPA
328	101	53	245
338	138	69	253
348	152	81	256

[a] Abbreviation E used for eugenol.

It is well known that DMPA works according to a fast α-cleavage process. It produces primarily benzyl and dimethoxybenzoyl radicals (Scheme I).[23] The latter undergoes a fast demethylation and yields free methyl radicals that can partici-

Table III Evaluation of Total Enthalpy Change, ΔH_g, of TMPTA Photopolymerization at 383 K (Parameters *A* and *B* are used in Eq. 3)

System	Value of Parameter *A*	Value of Parameter *B*	ΔH_g Calculated at 383 K (J g^{-1})
AIBN	—	—	408[a]
BP/MDEA	11.8	2360	281
BP/MDEA + E[b]	11.6	2490	163
DMPA	6.27	252	274

[a] Value measured directly at 383 K.
[b] Abbreviation E for eugenol.

pate in the initiation step. Such cleavable photoinitiators possess a short-lived triplet state that is not affected by monomer or impurity quenchings. The triplet lifetime of DMPA is under 100 ps, and the cleavage rate constant is higher than 10^{10} s^{-1}.[23] Quenching this state by phenols would require both a high-rate constant and a high concentration in phenols in order to compete with the cleavage. Such a behavior is not observed even when quenching with amines,[23] while the photoreduction of carbonyl triplets by these compounds occurs with rate constants close to the diffusion limit. Thus, it is reasonable to postulate that phenols do not quench the triplet state of DMPA. This point is relevant because of the lack of retardation or inhibition effects noticed in DSP experiments. However, it is necessary to check that phenols do not react with initiating radicals released by photocleavage.

The lifetime of ^{3}BP is in the range of several microseconds in many solvents. It allows quenching by chemicals such as alcohols, aromatic compounds, or amines.[24,25] For instance, a quenching rate constant of 3×10^9 M^{-1} s^{-1} has been found with MDEA in MMA 7 mol L^{-1}.[23] This high value is quite representative of the quenching by amines. The concentration of MDEA was 2×10^{-2} mol L^{-1} in our experiments. It is thus obvious that if phenols are able to quench ^{3}BP as fast as amines and if the concentration of phenolic constituents in the coating can be near the concentration of MDEA, then these phenols open a new competitive way of deactivation of the triplet state. Thus two hypotheses that arose from the DSP experiments explain the retardation effect observed with the BP–MDEA photoinitiating system: (1) the retardation is due to the quenching of ^{3}BP by phenols and (2) phenols are able to scavenge the primary radicals produced by the photoreduction of BP by MDEA.

Role of Phenols in BP–MDEA Photoinitiating System

If phenolic compounds actually interact with ^{3}BP, a photoreduction process by hydrogen abstraction, which produces ketyl and phenoxyl radicals, can be considered. Indeed, it is well known that excited aromatic ketones abstract hydrogen from many substrates, such as hydrocarbons, alcohols, and amines.[24,25] Two mechanisms are commonly invoked to rationalize these experimental facts. First, a direct hydrogen atom abstraction has been proposed, which accurately applies in the case of aliphatic hydrocarbons.[26] The homolytic bond breaking favors aromatic ketones with n, π^* states as revealed by a study of quenching rate constants and radical quantum yields. There is experimental evidence that in that case carbonyl n, π^* triplet state behaves much like alkoxy radicals.[27] The quenching rate constants for direct hydrogen atom abstraction span the range of 10^4–10^6 M^{-1} s^{-1}.[28,29]

A second mechanism is required when aromatic hydrocarbons and compounds with a low oxidation potential, such as amines, quench carbonyl triplets. In that case, an increase of reactivity can be observed, with the quenching-rate constants rising to 10^9–10^{10} M^{-1} s^{-1}.[30] The efficiency of hydrogen transfer also increases since, for instance, the radical quantum yield approaches unit with amines. Several experimental facts suggest a two-step process that may compete with homolytic atom transfer. The first step is a "partial" or a "full" electron transfer, producing an "*exciplex*" (excited charge transfer complex) or an ion pair, followed by a hydrogen atom or a proton migration. Supporting this mechanism is that the harder it is to reduce ketones, the lower is the reactivity.[31] This second mechanism is invoked with amines but also with phenols, since it was

Table IV Quenching Rate Constants, k_Q, of ^{3}BP by Phenolic Derivatives and Ketyl Radical Quantum Yields Φ_{RAD}

Substituted Phenols	$k_Q \times 10^9$ (M^{-1} s^{-1})	Φ_{RAD}
Phenol	0.34	0.52
Guaiacol	1.2	0.54
Eugenol	2.0	0.63
2,6-Dimethoxyphenol	3.0	0.38
Catechin	3.2	0.56
Gallic Acid	3.2	0.52
Syringic Acid	3.4	0.5
Vanillin	6.4	0.54
t-4-Hydroxystilbene[a]	6.7	—
Syringaldehyde	7.0	0.4
Sinapinic Acid[a]	7.6	—
Coniferylaldehyde[a]	12	—

Solvent is acetonitrile, temperature is 25°C.
[a] Not determined due to absorption of phenol at 355 nm.

shown in 1981 that phenols quench aromatic carbonyl triplets in a very fast process for both the n, π^* and π, π^* states.[32] The quenching-rate constants obtained range from 10^9 to 10^{10} M^{-1} s^{-1}. It was concluded that the reaction implies a charge–transfer intermediate, with ketone as the electron acceptor and phenol the electron donor. It was also demonstrated that the photoreduction process leads to phenoxyl and ketyl radicals with significant but under-unit quantum yields.

Quenching Rate Constants and Radical Ketyl Quantum Yields

Table IV summarizes the rate constants k_Q of the quenching of ^{3}BP by the 12 phenolic compounds studied in this work. Nearly all the values stayed in the range of 10^9–10^{10} M^{-1} s^{-1}, indicating a strong interaction between phenols and the carbonyl triplet. The formation of ketyl radicals detected in these experiments confirms that a hydrogen abstraction occurs between ^{3}BP and phenols. Phenoxyl radicals usually absorb around 400–420 nm[27,32] but the overlap with the residual absorption of BPH• and the lack of absorption band for several phenoxyls prevent us from using it to calculate the radical quantum yield. A typical evolution of Φ_{RAD} with quencher concentration is shown in Figure 4. The deactivation of the carbonyl triplet state increases with the quencher concentration and nearly reaches the rate of maximal actual ketyl quantum yield—hence the plateau observed. No decrease of this plateau value by increasing quencher concentration was noticed until a concentration of 0.1 mol L^{-1} of phenols was reached. So it was kept as the actual quantum yield of the photoreduction process. Values of Φ_{RAD} are listed in Table IV. The radical quantum yield is about the same from one phenol to another and is significantly under unit (about 0.5). These data support the trend observed with the k_Q values, that is, the dramatic homogeneity of the reactivity of the phenols studied, however varied their chemical structures.

Redox Potentials

For all compounds, the shape of the cyclic voltammograms and their evolution with the sweep rate indicate an irreversible behavior at the gold or platinum electrodes. The platinum electrode was finally used in order to allow the measurement of the oxidation peak potential of phenol itself, which was not possible with the gold electrode. The irreversibility of the voltammograms only allowed measurement of the peak oxidation potentials, E_p, of all the phenols studied. The sweep rate was fixed at 1 V s^{-1}; this was the best working condition to determine the high peak values of phenol and vanillin. The E_p potentials were used to choose a correct range of potential to perform RDEV. The values of the half-wave oxidation potential, $E_{1/2}$, are less sensitive to the sweep rate and concentration than that in CV and can be taken as a rather good approximation of the standard oxidation potentials.

The E_p and $E_{1/2}$ potentials of the 12 phenols are listed in Table V. The $E_{1/2}$ oxidation poten-

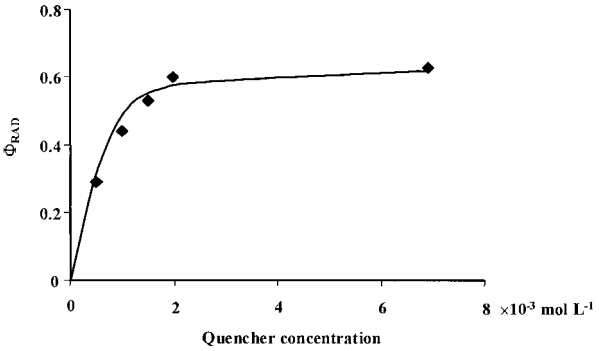

Figure 4 A typical evolution of the ketyl radical quantum yield Φ_{RAD} with the concentration of phenolic quencher. [BP] = 5×10^{-3} mol L^{-1}, quencher used is eugenol, solvent is acetonitrile, and temperature is 25°C.

Table V Peak (E_p) and Half-Wave ($E_{1/2}$) Oxidation Potentials of Phenols

Substituted Phenols	E_p (V/SCE)	$E_{1/2}$ (V/SCE)
Phenol	1.84	1.68
Guaiacol	1.48	1.32
Eugenol	1.44	1.22
2,6-Dimethoxyphenol	1.26	1.16
Catechin	1.28	1.17
Gallic Acid	1.45	1.14
Syringic Acid	1.64	1.33
Vanillin	1.69	1.51
t-4-Hydroxystilbene	1.22	1.09
Syringaldehyde	1.52	1.31
Sinapinic Acid	1.41	1.17
Coniferylaldehyde	1.44	1.27

Solvent is acetonitrile, supporting electrolyte is 0.1 mol L^{-1} *tert*-butylammonium hexafluorophosphate, and temperature is 25°C.

tials span from +1.09 V/SCE for *trans*-4-hydroxystilbene to +1.68 V/SCE for phenol. The peak potentials measured for guaiacol and 2,6-dimethoxyphenol (1.48 and 1.26 V/SCE, respectively) are in good agreement with the values recently found in benzonitrile solutions using a platinum electrode (respectively, 1.41 and 1.27 V/SCE[33]). However, $E_{1/2}$ values rather than E_p values, were used preferentially to characterize the oxidation properties of phenolic derivatives because they had the lowest sensitivity to experimental conditions. This approach represents a consistent determination of the oxidation properties inside the set of phenols studied.

Some Considerations on the Quenching Mechanism

As said above, the quenching-rate constants are near the diffusion-rate constant, considerably higher than expected in a homolytic bond breaking. No charged intermediate species, which would have supported a sequential electron/proton transfer mechanism, was detected in the NTA experiments. However, the high values of the quenching-rate constants and their similarity to those obtained with amines (for which there is evidence of intermediate charged species[20,34]) show that phenolic hydrogen transfer to carbonyl triplets is more complex than a simple atom migration. The similar quenching-rate constants of phenols and amines suggest that an electron transfer may be involved in the photoreduction process. The study of the reaction in a picosecond or femtosecond time scale would bring some interesting information about the mechanism of the photoreduction of BP by phenols. Surprisingly, to our knowledge there are no such experiments described in the literature, while hydrogen transfer reaction with amines is greatly detailed. If the mechanism involves a charge transfer, the thermodynamics of the reaction should be reflected[35,36] by eq. (4):

$$\Delta G_{ET} \cong E(D/D^+) - E(A^-/A) - E_T + C \quad (4)$$

where ΔG_{ET} is the free energy change of electron transfer between the aromatic carbonyl triplet of energy E_T and the phenolic electron donor; $E(D/D^+)$ is the oxidation potential of the latter, while $E(A^-/A)$ is the reduction potential of the ground state ketone; and C is a coulombic term that takes into account the electrostatic interaction within the resultant radical ion pair.

Figure 5 plots the curve of log k_Q versus ΔG_{ET} calculated by eq. (4) with the $E_{1/2}$ potentials of phenolic derivatives. Figure 5 also shows the empirical Rehm–Weller curve,[37] which is known to describe the evolution of the experimental electron transfer rates with the free energy change of the electron transfer process. The following data for BP were used: $E(A^-/A) = -1.76$ V/SCE,[38] E_T

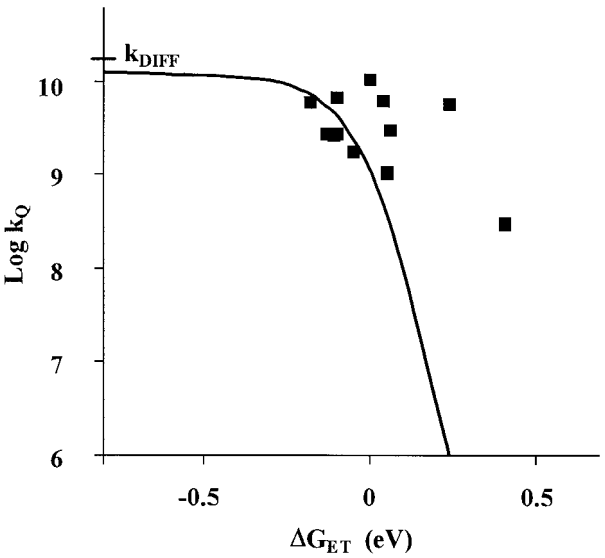

Figure 5 Plot of log k_Q versus ΔG_{ET} for BP. ΔG_{ET} is calculated with eq. (4) using the $E_{1/2}$ oxidation potentials (see text). Solvent is acetonitrile; temperature is 25°C. The Rehm–Weller curve is calculated with the parameters of reference 37.

= 2.96 eV.[39] C was taken as −0.06 eV, the usual value for polar media like acetonitrile.[37] It is clear that quenching-rate constants are higher than expected, and do not follow the Rehm–Weller curve. Indeed, Figure 5 indicates that despite their relatively high oxidation potentials, phenols strongly interact with ^{3}BP, the thermodynamics of this interaction not reflected by eq. (4). This shows that hydrogen abstraction with phenols does not involve a pure electron transfer. Even though the quenching-rate constants are not relevant to the oxidation properties of phenols, their diffusion-close values rule out a direct hydrogen atom abstraction, with an alkoxy radical-like behavior of the n, π^* triplet state of BP.

It thus appears that the two common mechanisms (direct hydrogen atom abstraction and sequential electron and proton transfer) fail to describe the photoreduction of BP by phenols. From looking at the quenching in acetonitrile of several substituted benzophenones by p-cresol, a new mechanism has been recently proposed that takes into account the nucleophilic role of ketone and thus its acid–base properties.[40] The electron-acceptor-substituted benzophenones have shown an electrophilic behavior that is relevant to the mechanism involving a full or a partial electron transfer followed by a proton or a hydrogen atom transfer. However, the electron-donor substitution has brought about a reversed role for ketone. By increasing the electron-donor capability of the substituents, the carbonyl triplet moves to adopt a nucleophilic role inside the reaction. The hydrogen abstraction is then initiated by a partial or a total transfer of the phenolic proton to the carbonyl triplet, producing a hydrogen-bonded exciplex or an ion pair. Next, the electron is transferred within this intermediate. It has been emphasized[40] that the migration of the phenolic proton toward the carbonyl triplet gradually changes the redox properties of the two reactants until the free enthalpy change of electron transfer through the hydrogen bond becomes favorable. The photoreduction process then mainly depends on the triplet carbonyl redox and acid–base properties rather than the characteristics of the phenol. This is quite relevant to our kinetic data, which are quite homogeneous despite the relatively wide scale of the oxidation potentials and structural changes among the set of phenols studied in our work. It also explains the inability of eq. (4) to describe the thermodynamics of the reaction if the unprotonated BP were used. Indeed, ΔG_{ET} calculated for the electron transfer between the protonated carbonyl triplet and the phenoxide ion becomes strongly exergonic.[40] The effect of protonation is to induce a shift toward negative ΔG_{ET} values, which likely renders the reaction more exergonic than that calculated by eq. (4).

Detection of Phenoxyl Radicals by EPR Experiments

NTA experiments have provided evidence of the formation of BPH• in acetonitrile solutions. Phenols reduce BP efficiently and thus must be involved in the photoinitiation process of the UV curing of a wood coating. Some EPR experiments have been made directly on wood samples in order to detect the formation of phenoxyl radicals during irradiation and confirm that a photoreduction occurs at the wood surface. The samples are impregnated by a water–acetone solution containing photoinitiators that produce free radicals under UV irradiation. The three photoinitiating systems studied in this section were DMPA, BP–MDEA, and benzoinisopropylether (BIE). The reference used was a wood sample impregnated with the solvent alone.

The reference sample before UV irradiation gives an EPR singlet signal of low intensity and is shown in Figure 6. Its position relative to the signal of DPPH• is at $g = 2.004$, and its peak-to-peak line width is $\Delta H = 9.1$ G. Prior to irradiation the concentration of radicals is then sufficient to give an EPR signal. This observation has been already made with other wood species.[41] Ambient light absorption brings about a photodegradation of lignin present at the wood surface.[42] This degradation produces phenoxyl radicals by hydrogen abstraction or chemical bond breaking. A stationary concentration of phenoxyl radicals can thus be observed by EPR without specific UV irradiation. These radicals are responsible for the yellowing of wood pulp exposed to sunlight.[43] They give the EPR initial intensity, I_0, defined in the experimental section. After irradiation the intensity of this signal increases. No change was observed concerning its shape and g or ΔH values. The UV light absorption (with $\lambda > 310$ nm) increases the formation of such radicals because the intensity of the UV lamp is greater and the wavelengths are shorter than in ambient light.

Table VI summarizes the results concerning the EPR signal of phenoxyl radicals found for the two wood species and the three photoinitiating systems. Two concentrations for each photoinitiator were studied. It is clear that both benzoin derivatives (BIE and DMPA) are quite homoge-

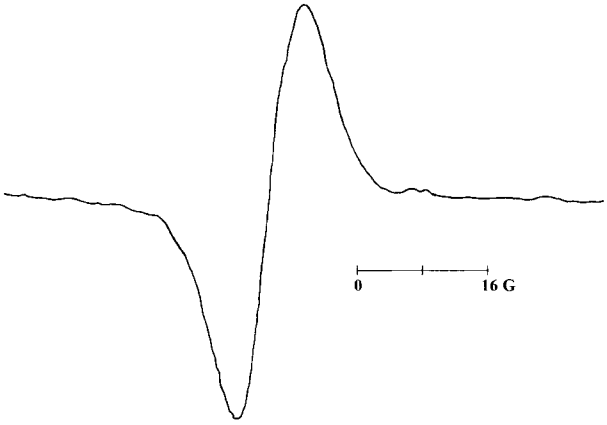

Figure 6 A typical first-derivative EPR spectra of phenoxyl radicals obtained for an European spruce wood sample coated with TMPTA. This signal was recorded prior to UV irradiation, showing the phenoxyls produced by the sunlight exposure and released by the photodegradation of lignin and other polyphenolic constituents. Measurement was at room temperature (about 21°C).

neous and give parameters ρ and k in good agreement with those for reference samples. At a high concentration DMPA diminishes I_0 and I_∞. It would seem that DMPA absorbs a part of the UV light and decreases the creation of phenoxyl radicals due to the photodegradation of lignin. The BP–MDEA system behaves quite differently. The ρ values are several times higher than those for benzoin derivatives. With maple, ρ reaches 7.3. I_0 increases with the concentration of the photoinitiating system. The triplet state of BP interacts with phenolic derivatives at the wood surface and produces ketyl and phenoxyl radicals. The growth of ρ means this new source of radicals is more productive than the photodegradation of lignin and wood extracts. These results are relevant to the DSC–DSP and NTA experiments. They confirm that phenolic derivatives react *in situ* with ^{3}BP, produce ketyl and phenoxyl radicals, and as a consequence create a new way of triplet deactivation that can inhibit or retard the polymerization of acrylates even without oxygen.

Interactions between Initiating Free Radicals and Phenols

The above experiments have provided evidence of the photoreduction of ^{3}BP by phenolic derivatives. However, the retardation effect observed in DSP experiments with the BP–MDEA photoinitiating system could be due to the interaction of phenols with some initiating radicals. Phenolic derivatives have a well-known antioxidant activity,[44] and the possible interaction between these latters and some radicals formed in the initiating step of photopolymerization must be taken into account. Three monophenols (phenol, 2,6-dimethoxyphenol, and guaiacol) were selected for their low absorption at 355 nm in order to study through NTA experiments their interaction with some radicals released by the photocleavage of DMPA and the photoreduction of BP by MDEA.

Table VI EPR Parameters for Wood Samples Coated with Photosensitive Formulations

Wood Species	Gain	Sample[a]	I_∞ (Arbitrary Unit)[b]	I_0 (Arbitrary Unit)[b]	ρ[b]	$k \times 10^3$ (s^{-1})[b]
Norway maple	1.25×10^6	Reference	31.2	18.5	0.69	1.03
		3% DMPA	32.0	17.7	0.80	1.03
		25% DMPA	15.8	11.2	0.41	0.72
		3% BIE	31.5	18.3	0.72	1.18
		15% BIE	32.8	19.0	0.72	1.35
European spruce	1.25×10^6	Reference	35.7	17.9	1.00	1.34
		3% DMPA	34.5	19.0	0.82	1.50
		25% DMPA	29.3	17.9	0.64	0.79
		3% BIE	30.9	17.4	0.77	1.15
		15% BIE	29.4	19.4	0.51	1.33
Norway maple	2.5×10^5	3% BP–MDEA	18.6	3.6	4.1	1.06
		10% BP–MDEA	44.0	5.3	7.3	1.23
European spruce	2.5×10^5	3% BP–MDEA	17.6	3.5	4.0	0.90
		10% BP–MDEA	22.1	5.6	3.0	0.96

Solvent used for impregnation is a mix of water–acetone (v/v 30–70).
[a] Percentages in weight.
[b] See experimental section for definition of parameters.

Interaction with Benzoyl and Benzyl Radicals

The photocleavage of DMPA produces benzoyl and α,α-dimethoxybenzyl radicals (Scheme I). The latter undergoes next a fast demethylation.[23] The interaction of phenols with benzoyl and α,α-dimethoxybenzyl radicals was studied for this section. The transient absorption decay of the latter radical was followed at 410 nm, its maximum absorption band.[45,46] The decay of the benzoyl radical was recorded at 370 nm.[45] The yield of scavenging Φ_S of the transient radicals is given by eq. (5):

$$\Phi_S = 1 - \frac{1}{1 + k_R\tau_0[\mathrm{ArOH}]} \qquad (5)$$

where [ArOH] is the concentration of phenol in mol L^{-1}, k_R the rate constant between radicals and phenols, and τ_0 the lifetime of radicals without phenols. Under our working conditions Φ_S was estimated to be less than 0.1, even with the addition of 1 mol L^{-1} of phenol, guaiacol, or 2,6-dimethoxyphenol. The possible quenching-rate constant, k_R, of these radicals by monophenols is thus estimated to be less than 2×10^3 M^{-1} s^{-1}, regarding the lifetime τ_0 of the radicals (about 60 μs).

Interaction with BPH•

The possible interaction of phenols with BPH• was also studied. First ^{3}BP was quenched with a small amount of a phenolic compound to determine the lifetime of the ketyl radical produced. A second-order kinetic law was used to fit the curves. After that, more phenol was added, and the ketyl lifetime was determined again by a second-order and a first-order kinetic. If phenols react with ketyl radicals, the kinetic should gradually change from second to pseudo-first order, and its lifetime should decrease. Figure 7 shows the effect of the addition of 0.6 mol L^{-1} of phenol on the ketyl transient absorption at 545 nm, compared to the signal with a lower concentration of phenol (0.017 mol L^{-1}). It can be seen that phenol does not scavenge efficiently the ketyl radical. With guaiacol and 2,6-dimethoxyphenol the same conclusions were drawn. Φ_S for BPH• was estimated to be under 0.1. The lifetime of BPH• in the presence of about 0.5 mol L^{-1} of phenols is 20 μs; this gives a maximal rate constant, k_R, of ketyl radicals scavenging of 3×10^4 M^{-1} s^{-1}.

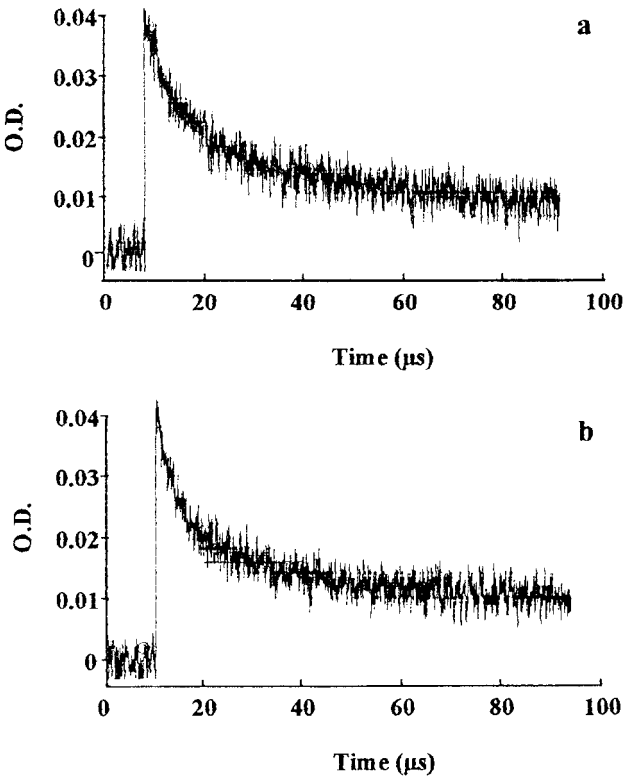

Figure 7 Kinetic decay of the transient absorption of the ketyl radical at 545 nm: (a) with 0.017 mol L^{-1} of phenol, (b) with 0.6 mol L^{-1} of phenol. Solvent is acetonitrile; measurement was at room temperature (about 25°C).

CONCLUSION

Phenols greatly react with carbonyl triplet of aromatic ketones. A typical quenching-rate constant value is 3×10^9 M^{-1} s^{-1}. The reaction produces ketyl and phenoxyl radicals. Transient absorption experiments allow us only to detect ketyl radicals. The quantum yield of the photoreduction has been found to be around 0.5 in acetonitrile. The mechanism is unclear, but direct hydrogen atom abstraction can be ruled out in view of the values of k_Q.

No charged intermediate species has been detected by nanosecond transient absorption spectroscopy. Therefore, on this time scale, there is no direct evidence that could support a sequential electron/proton transfer mechanism. The unusual reactivity of phenol regarding its high oxidation potential cannot be well described by eq. 4 and cannot be thermodynamically controlled by the electron transfer step, even though a charge transfer is suggested by the high k_Q values.

The EPR experiments have shown that phenoxyl radicals are produced in a noticeable amount when the photopolymerization is made with the BP–MDEA system. They confirm that the photoreduction of BP by phenolic derivatives occurs and open a new way of triplet deactivation.

This competitive way is inefficient for initiating the polymerization of TMPTA, confirmed by the decrease of ΔH_g with the addition of phenols in the case of the BP–MDEA system. It also explains the retardation effect observed in the DSP experiments. The study of a possible reaction between monophenols and radicals has shown that the reaction rate constant is under 2×10^3 M^{-1} s^{-1} with benzyl and benzoyl radicals released by the photocleavage of DMPA and under 3×10^4 M^{-1} s^{-1} with BPH•. The DSC–DSP experiments have shown that monophenols do not induce retardation effects, even at 0.05 mol L^{-1}. It thus seems that compounds with only one phenolic function and few substituents do not interact strongly with either initiating or monomeric radicals in our systems. The decrease of ΔH_g by adding monophenols is consistent with the well-known chain-breaking activity greatly involved in the antioxidant properties of phenolic derivatives.[44]

It is now possible to evaluate the consequences of the photoreduction of photoinitiators by phenolic derivatives inside a photosensitive formulation applied on a wood surface. The influence of phenols inside the photoinitiating step is compared in Schemes III and IV for the direct cleavage of DMPA and the two-component system BP–MDEA. M is the acrylate monomer used.

In Scheme III, k_C, k_I, k_P, k_R, and k_S are, respectively, the rate constants for the DMPA cleavage, the initiation step, the propagation step, and the scavenging of primary and monomeric radicals by the phenols ArOH. The possible interactions of phenols with polymeric radicals are not represented. Scheme III illustrates that phenols can not interact with the triplet state of DMPA due to the latter's very short lifetime[23] and its almost instantaneous cleavage. That is why the EPR signal of phenoxyl radicals is not significantly enhanced in photocuring formulations of wood coatings using benzoin ether photoinitiators. The low inhibition effect observed in the DSP experiments shows that phenols do not scavenge primary and monomeric radicals with high

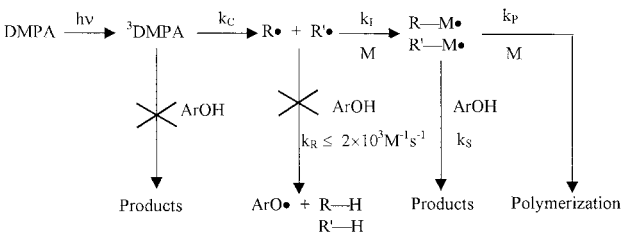

Scheme 3

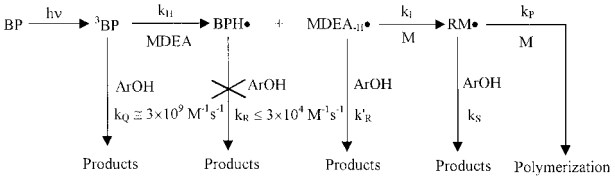

Scheme 4

rate constants. They only induce a decrease of the crosslinking of TMPTA by their chain-breaking activity toward polymeric radicals.

In Scheme IV, k_I, k_P, and k_S have the same significance; k_H and k_Q are, respectively, the rate constants for the hydrogen transfer between BP and MDEA and the quenching of ^{3}BP by phenols. Two rate constants for radical scavenging are indicated: k_R, for the scavenging of BPH•, and k'_R, for the scavenging of MDEA_H•. The main influence of phenols is represented by the relative values of k_H and k_Q. The initiating radical in Scheme IV is MDEA_H•. If phenols are present, the creation of this radical is decreased by a factor of η, given by eq. (6):

$$\eta = \frac{k_H[\text{MDEA}]}{k_H[\text{MDEA}] + k_Q[\text{ArOH}]} \tag{6}$$

The average rate constant between ^{3}BP and the phenolic derivatives studied in this paper is 3×10^9 M^{-1} s^{-1}. The value of k_H is also 3×10^9 M^{-1} s^{-1}.[23] Taking a usual value of [MDEA] equal to 0.1 mol L^{-1}, η is easily calculated to be 0.5 for [ArOH], equal to 0.1 mol L^{-1}. It is clearly very difficult to estimate the concentration of phenolic derivatives in the wood coating during the irradiation. However, it seems reasonable that wood species rich in phenolic constituents, such as maple or spruce, can release phenols in the coating with a sufficient concentration to significantly interact with ^{3}BP. In addition to this primary effect, the photoreduction of the triplet state by phenols produces ketyl radicals that are known to be chain terminators and to negatively influence the propagation step.[47]

In conclusion, phenols have little effect on the polymerization of TMPTA initiated by a thermal or a fast photocleavable initiator. On the contrary, the experiments seem likely to indicate that the noticeable retardation effect obtained with the two-component BP–MDEA system is brought about by a competition between MDEA and phenols to deactivate ^{3}BP. This latter reacts greatly with phenols, but contrary to MDEA, the

deactivation does not produce radicals able to initiate the polymerization process, hence the resulting decrease of crosslinking observed by DSP. It has been shown by EPR that phenoxyl radicals are created *in situ* during the irradiation of the wood coating. This confirms that the phenolic molecules present in wood and released inside the coating follow the same behavior toward ^{3}BP rather than the phenolic models studied in our work. Further work will be done to determine precisely and to quantify the role of the chemical structure of phenols on the retardation effect. It has been decided that some of these studies will use polymeric molecules such as tannins.

REFERENCES

1. Baumann, H.; Timpe, H. J. Kunstoffe 1989, 79 (8), 696.
2. Fisher, W.; Uerdingen, B. Ind Lackierbetr 1993, 2, 54.
3. Kostelnik, R. Radtech Rep 1994, 8 (4), 16.
4. Dufour, P. In Radiation Curing in Polymer Science and Technology Volume I; Fouassier, J.-P.; Rabek, J. F., Eds.; Elsevier Science: New York, 1993; p. 1.
5. Li Bassi, G. In Radiation Curing in Polymer Science and Technology Volume II; Fouassier, J.-P.; Rabek, J. F., Eds.; Elsevier Science: New York, 1993; p. 239.
6. Chatton, P. Surf Coat Int 1995, 78 (11), 486.
7. Stoye, D.; Freitag, W. In Resins for coatings; Stoye, D.; Freitag, W., Eds.; Hanser Publishers, 1996.
8. Zav'yalov, A. N.; Kasilova, L. V. Soversh Term Pererab Drevesiny 1980, M, 35.
9. Zav'yalov, A. N.; Kasilova, L. V. Lesokhim Podsochka 1978, 8, 13.
10. Zav'yalov, A. N.; Kasilova, L. V.; Aseeva, Z. G. Gidroliz Lesokhim Prom-st 1982, 5, 12.
11. Barabashina, R. A.; Sporsheva, E. I.; Fomin, V. A.; Toporkova, I. A.; Kharitonova, V. M.; Shatskaya, T. F. Khim Prom-st 1984, 5, 87.
12. Mibayashi, S.; Masao, M.; Yasuhiko, K.; Yokota, T. Mokuzai Gakkaishi 1982, 28 (12), 795.
13. Mibayashi, S.; Watanabe, T.; Yokota, T. Mokuzai Gakkaishi 1983, 29 (10), 695.
14. Mibayashi, S.; Yokota, T. Mokuzai Gakkaishi 1984, 30 (1), 55.
15. Fujisawa, S.; Kadoma, Y. Dent Mater 1992, 8, 324.
16. Enmanji, K. Bull Chem Soc Jpn 1985, 58, 2181.
17. Wight, F. R. J Polym Sci: Polym Lett Ed 1978, 16, 121.
18. Wight, F. R.; Nunez, I. M. J Radiat Curing 1989, 16, 3.
19. Godfrey, T. S.; Hilpern, J. W.; Porter, G. Chem Phys Letters 1967, 1, 490.
20. Miyasaka, H.; Morita, K.; Kamada, K.; Mataga, N. Bull Chem Soc Jpn 1990, 63, 3385.
21. Fengel, D.; Wegener, G. Wood Chemistry, Ultrastructure, Reactions; De Gryyter, W., Ed.; Berlin, 1984.
22. Godard, V. Ph.D. Thesis, Université Henri Poincaré-Nancy, 1998.
23. Fouassier, J.-P. Photoinitiation Photopolymerization and Photocuring; Hanser Publishers, 1995; Chapter 1, p. 20.
24. Scaiano, J. C. J Photochem 1973–74, 2, 81.
25. Wagner, P. J. Topics in Current Chemistry 1976, 66, 1.
26. Griller, D.; Howard, J. A.; Marriott, P. R.; Scaiano, J. C. J Am Chem Soc 1981, 103, 619.
27. Das, P. K.; Encinas, M. V.; Steenken, S.; Scaiano, J. C. J Am Chem Soc 1981, 103, 4162.
28. Wolf, M. W.; Brown, R. E.; Singer, A. L. J Am Chem Soc 1977, 99:2, 526.
29. Giering, L.; Berger, M.; Steel, C. J Am Chem Soc 1974, 96, 953.
30. Inbar, S.; Linschitz, H.; Cohen, S. G. J Am Chem Soc 1981, 103, 1048.
31. Wagner, P. J.; Truman, R. J.; Puchalski, A. E.; Wake, R. J Am Chem Soc 1986, 108, 7727.
32. Das, P. K.; Encinas, V.; Scaiano, J. C. J Am Chem Soc 1981, 103, 4154.
33. Biczok, L.; Gupta, N.; Linschitz, H. J Am Chem Soc 1997, 119, 12601.
34. Devadoss, C.; Fessenden, R. W. J Phys Chem 1991, 95, 7253.
35. Weller, A. Pure & Applied Chem 1968, 16, 115.
36. Guttenplan, J. B.; Cohen, S. G. J Am Chem Soc 1972, 94, 4040.
37. Rehm, D.; Weller, A. Isr J Chem 1970, 8, 259.
38. Jacques, P.; Allonas, X.; Von Raumer, M.; Suppan, P.; Haselbach, E. J Photochem Photobiol A: Chem 1997, 111, 41.
39. Leigh, W. J.; Arnold, D. R. J Chem Soc, Chem Commun 1980, 406.
40. Leigh, W. J.; Lathioor, E. C.; Saint-Pierre, M. J. J Am Chem Soc 1996, 118, 12339.
41. Martin, F. Ph.D. Thesis, Université Henri Poincaré-Nancy 1, 1996.
42. Hon, D. N. S. J Appl Polym Sci 1984, 29, 2777.
43. Heitner, C. In Photochemistry of Lignocellulosic Materials; Heitner, C.; Scaiano, J. C., Eds.; ACS Symposium Series 531, 1993.
44. Burton, G. W.; Hughes, L.; Ingold, K. U. J Am Chem Soc 1983, 105, 5950.
45. Fischer, H.; Baer, R.; Verhoolen, I.; Walbiner, M. J Chem Soc Perkin Trans 2 1990, 787.
46. Huggenberger, C.; Lipscher, J.; Fischer, H. J Phys Chem 1980, 84, 3467.
47. Block, H.; Ledwith, A.; Taylor, A. R. Polymer 1971, 12, 271.